

See discussions, stats, and author profiles for this publication at: <https://www.researchgate.net/publication/281779949>

Monolayer to Interdigitated Partial Bilayer Smectic C Transition in Thiophene-Based Spacer Mesogens: X-ray Diffraction and ^{13}C Nuclear Magnetic Resonance Studies

ARTICLE *in* LANGMUIR · SEPTEMBER 2015

Impact Factor: 4.46 · DOI: 10.1021/acs.langmuir.5b02327

READS

57

6 AUTHORS, INCLUDING:



E. Varathan

Central Leather Research Institute

16 PUBLICATIONS 46 CITATIONS

SEE PROFILE



Nitin P Lobo

Central Leather Research Institute

18 PUBLICATIONS 76 CITATIONS

SEE PROFILE



Arun Roy

Raman Research Institute

36 PUBLICATIONS 335 CITATIONS

SEE PROFILE

Monolayer to Interdigitated Partial Bilayer Smectic C Transition in Thiophene-Based Spacer Mesogens: X-ray Diffraction and ^{13}C Nuclear Magnetic Resonance Studies

M. Kesava Reddy,[†] E. Varathan,[‡] Nitin P. Lobo,^{¶,||} Arun Roy,[⊥] T. Narasimhaswamy,[§] and K. V. Ramanathan^{*,#}

[†]Department of Chemistry, S. V. University, Tirupati, 517502, India

[‡]Chemical Laboratory and [§]Polymer Laboratory, CSIR-Central Leather Research Institute, Adyar, Chennai 600020, India

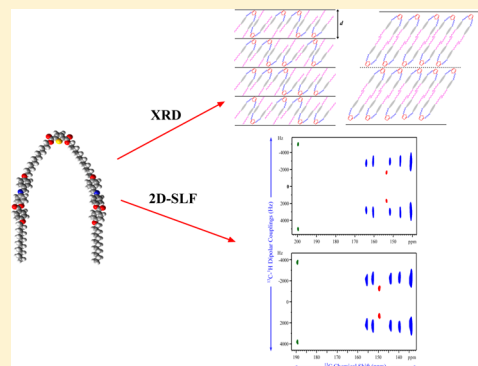
^{||}Department of Physics, Indian Institute of Science, Bangalore, 560012, India

[⊥]Soft Condensed Matter, Raman Research Institute, Bangalore, 560080, India

[#]NMR Research Centre, Indian Institute of Science, Bangalore, 560012, India

Supporting Information

ABSTRACT: Mesophase organization of molecules built with thiophene at the center and linked via flexible spacers to rigid side arm core units and terminal alkoxy chains has been investigated. Thirty homologues realized by varying the span of the spacers as well as the length of the terminal chains have been studied. In addition to the enantiotropic nematic phase observed for all the mesogens, the increase of the spacer as well as the terminal chain lengths resulted in the smectic C phase. The molecular organization in the smectic phase as investigated by temperature dependent X-ray diffraction measurements revealed an interesting behavior that depended on the length of the spacer *vis-a-vis* the length of the terminal chain. Thus, a tilted interdigitated partial bilayer organization was observed for molecules with a shorter spacer length, while a tilted monolayer arrangement was observed for those with a longer spacer length. High-resolution solid state ^{13}C NMR studies carried out for representative mesogens indicated a U-shape for all the molecules, indicating that intermolecular interactions and molecular dynamics rather than molecular shape are responsible for the observed behavior. Models for the mesophase organization have been considered and the results understood in terms of segregation of incompatible parts of the mesogens combined with steric frustration leading to the observed lamellar order.



INTRODUCTION

Molecular mesogens containing flexible spacers commonly known as dimers, trimers, and oligomers have gained importance in view of their unusual mesophase characteristics as well as their structural resemblance to mesogenic polymers.^{1–4} The construction of dimers/oligomers follows the principle of connecting two or more rigid cores through flexible spacers with terminal alkoxy chains at both the ends.^{5,6} The remarkable feature of these dimers/oligomers in contrast to conventional low molar mass mesogens (calamitic mesogens) is the dependency of mesophase characteristics on the length and the parity of the spacer.^{1–6} The recent past witnessed growing interest in symmetric and nonsymmetric trimers in which the flexible spacer is connected to the central rigid unit.^{7–11} These mesogens differ from the classical dimers in the sense that the center part of the mesogen is made up of an anisometric rigid ring rather than a flexible methylene unit often employed for realizing dimers. Among the nonsymmetric trimers, those based on central phenyl ring draw particular interest as the variation in the location of spacer on the phenyl

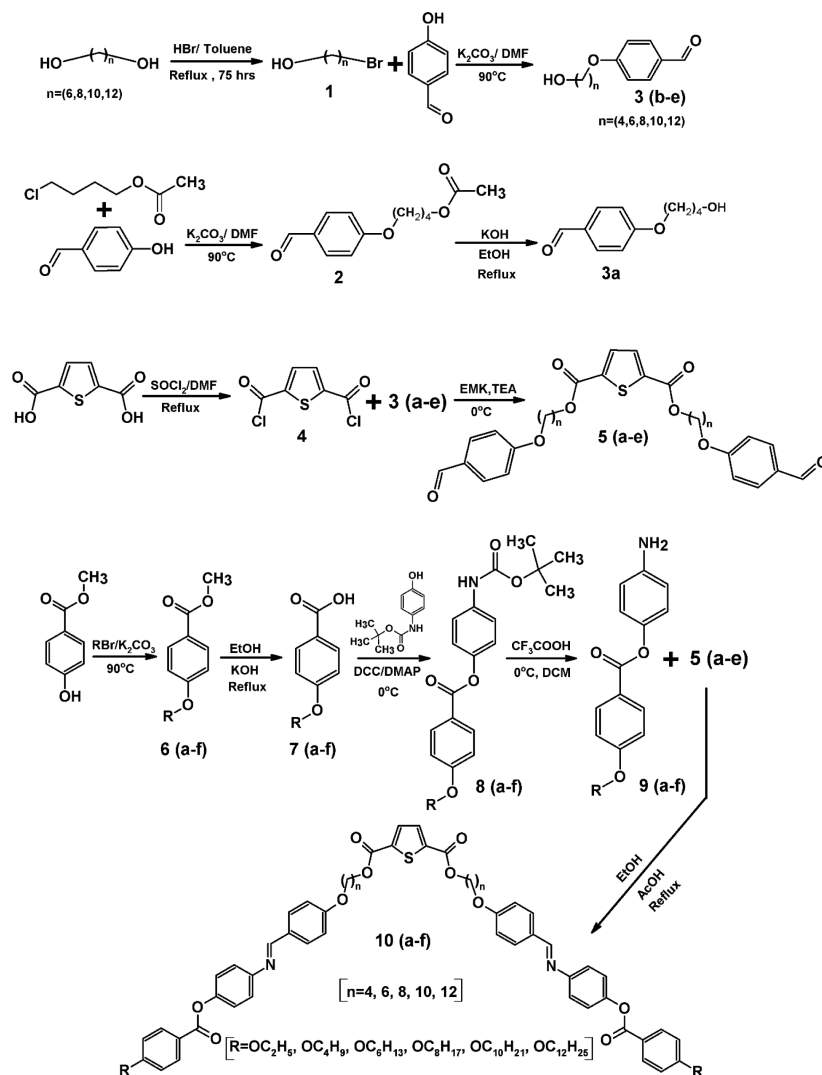
ring would result in a variety of molecular architectures, namely, star-like, bent-core, λ , and T-shaped mesogens.^{12–16} Depending on the spacer length as well as the length of the rigid core, a wide range of mesophase morphologies like nematic, smectic, banana, and columnar phases have been realized.^{17,18} In this scenario, it will be interesting to investigate mesogens containing five-membered heterocyclic systems in the spacer unit. Even though five-membered heterocyclic rings have made significant inroads into the armory of calamitic mesogens as core units,^{19–22} to the best of our knowledge, investigations on spacer containing mesogens with five ring moiety at the center have not been explored so far. The recent observation of biaxial nematic phases in oxadiazole centered mesogens has fuelled significant interest in five-membered heterocyclic systems, and, accordingly, many molecular mesogens have appeared in the literature.^{23–26} In this work, we have undertaken a

Received: June 25, 2015

Revised: August 19, 2015

Published: September 14, 2015

Scheme 1. Synthetic Strategy for the Target Mesogens



comprehensive characterization of a 2,5-thiophene dicarboxylate-based spacer containing mesogens in which the side arm is built with a core containing three phenyl rings and a terminal alkoxy chain. By varying the length of the spacer (4–12 even carbons) as well as the terminal chain length (2–12 even carbons), 30 molecules have been synthesized. The hot-stage polarizing microscopy (HOPM) and differential scanning calorimetry (DSC) studies have been employed to determine the transition temperatures of the synthesized mesogens. The molecular packing and organization have been examined by variable temperature powder X-ray diffraction (XRD). For two representative mesogens, high-resolution solid state ^{13}C NMR studies have been carried out, and the ordering and orientational behavior of different segments have been obtained. The investigations provide an insight into the liquid crystalline behavior in terms of the molecular shape and the influence of the length of the spacer on the molecular organization such as the monolayer versus the bilayer arrangement. It is anticipated that such investigations on conformationally sensitive mesogens could help to establish the molecular origin of self-assembly in liquid crystalline phases, which is of great fundamental interest.^{27,28}

EXPERIMENTAL SECTION

All the homologues of the series were synthesized by multistep route. The experimental protocols and the spectral data of the intermediates as well as final compounds are listed in the [Supporting Information](#). The molecular structures of mesogens were confirmed by Fourier transform infrared spectroscopy (FT-IR), and the spectra were recorded on an ABB BOMEM MB3000 spectrometer using KBr pellets. ^1H and ^{13}C NMR spectra of the compounds were recorded in CDCl_3 either on JEOL ECA 500 MHz or Bruker AV-III 400 MHz instrument at room temperature using tetramethylsilane as an internal standard. The resonance frequencies of ^1H and ^{13}C were 500.15 and 125.76 MHz for the former and 400.23 and 100.64 MHz for the later, respectively. The mesophase transitions such as melting and clearing temperatures were examined using Olympus BX50 HOPM equipped with a Linkam THMS 600 stage with a TMS 94 temperature controller. The DSC scans were carried out using a TA Q200 instrument with a heating rate of $10\text{ }^\circ\text{C}/\text{min}$ in nitrogen atmosphere.

Powder X-ray Diffraction Measurements. Variable-temperature X-ray diffraction measurements were carried out on unoriented samples filled in Lindemann capillary of diameter of 1 mm (Hampton Research, Aliso Viejo, CA) using $\text{Cu-K}\alpha$ ($\lambda = 1.54\text{ \AA}$) radiation from PANalytical instrument (DY 1042-Empyrean) and a linear detector (PIXcel 3D). The sample temperature was controlled with a precision of $0.1\text{ }^\circ\text{C}$ using a heater and a temperature controller (Linkam).²⁹

Computational Details. Density functional theory (DFT) has been used, and the ground state (S_0) geometrical optimization of S_{12} –

C_{12} mesogen in gas phase was carried out at the level of B3LYP/6-31G*.^{30,31} The NMR chemical shifts were calculated at the B3LYP/6-311+G(2d,p) level of theory using the gauge invariant atomic orbitals (GIAO) method to circumvent the gauge problem using B3LYP/6-31G(d) geometry.³² Cheeseman recommended the 6-311+G(2d,p) basis set for NMR chemical shifts after scrutiny of various basis sets, and hence the same was selected for the present study.³³ The scale factor determined for B3LYP/6-311+G(2d,p)//B3LYP/6-31G(d) methodology from the previous study was used for the calculation of ^{13}C NMR chemical shifts.³⁴ Accordingly, $d_{\text{scalc}} = 0.95d_{\text{calc}} + 0.30$, where d_{calc} and d_{scalc} are the calculated and the linearly scaled values of the ^{13}C chemical shifts, respectively. The chemical shift values of tetramethylsilane calculated at the same level of theory were used as the reference (182.5 ppm).³⁴ All calculations were carried out with the Gaussian 09 package.³⁵

Solid-State ^{13}C NMR Measurements. Solid-state ^{13}C NMR experiments were carried out in the smectic C and nematic mesophases for S_{12} – C_{12} and S_6 – C_{10} mesogens. For S_{12} – C_{12} mesogen, a Bruker Avance-III 500 WB NMR spectrometer was used, while for the S_6 – C_{10} , the experiments were carried out on Bruker Avance-III HD 400 WB NMR spectrometer. The resonance frequencies of ^1H and ^{13}C were 500.15 and 125.76 MHz for 500 MHz spectrometer and 400.07 and 100.61 MHz for the 400 MHz instrument (Supporting Information). The experiments in the liquid crystalline phases were performed using a static double resonance probe equipped with a 5 mm horizontal solenoid coil. ^{13}C NMR spectra were acquired by using standard Hartmann–Hahn cross-polarization pulse sequence with a contact time of 2 ms. Typical 90° proton pulse width for all the experiments was 4 μs . During carbon signal acquisition SPINAL-64,³⁶ decoupling was employed using a proton decoupling power of 30 kHz. A recycle delay of 8 s was used to avoid sample heating. Each spectrum was obtained typically with 512 scans. The 2D separated local field (SLF) NMR spectra under static condition at three different temperatures were obtained by using the SAMPI-4³⁷ pulse sequence shown in Scheme S1 of the Supporting Information. The earlier reports highlight the application of this pulse sequence to a variety of liquid crystalline systems.^{38,39} The method yields a 2D spectrum that correlates ^{13}C chemical shifts (F_2 dimension) with ^{13}C – ^1H dipolar oscillation frequencies (F_1 dimension). The SAMPI-4 experimental parameters were chosen as follows; contact time (τ): 3 ms, number of data t_1 points: 128, number of data t_2 points: 768, number of scans: 32, recycle delay: 12 s. The 2D data matrix is double Fourier transformed with 2k and 512 points in the F_2 and F_1 dimensions, respectively. A shifted sine bell window function was applied to the time domain data, and the spectrum was processed in the phase sensitive mode.

RESULTS AND DISCUSSION

The mesogens are constructed from 2,5-thiophene dicarboxylic acid, which is linked through a flexible methylene spacer to a rigid three phenyl ring side arm core and a terminal alkoxy chain. Scheme 1 shows the strategy adopted for synthesizing the mesogens. Interestingly, similar mesogens with two-phenyl ring side arm cores (Scheme S2 of the Supporting Information) failed to exhibit liquid crystalline property, which suggests that three-phenyl rings are essential to compensate the flexibility imparted by the spacer. The lengths of the spacer (4–12) and the terminal chain (2–12) were varied with an even number of carbons, and 30 homologues were realized. The mesogens are denoted as S_m – C_n series in which ‘m’ signifies the length of the spacer while ‘n’ represents that of the terminal alkoxy chain. In order to establish the relation between the structure of these mesogens and their liquid crystalline properties, a range of techniques are employed. The HOPM and DSC measurements are performed on the mesogens to characterize them in terms of the transition temperatures and the transition enthalpies. The HOPM studies also helped in identifying the presence of the tilted smectic phase in some of the mesogens. The

molecular organization of the mesophases is examined in detail by variable temperature powder X-ray diffraction. High-resolution solid state ^{13}C NMR studies are carried out in order to obtain insights into the molecular orientation as well as ordering. The magnitude and the orientation of dipole moments are calculated from the energy minimized structures using the DFT method.

The presence of flexible methylene spacer between the central thiophene ring and the side arm core can result in numerous conformations for the molecule. Out of these, three prominent energy minimized conformations leading to three different shapes are considered. A rod-like conformation representing linear dimers where both the arms are fully stretched is shown in Figure 1A. A U-shaped conformation

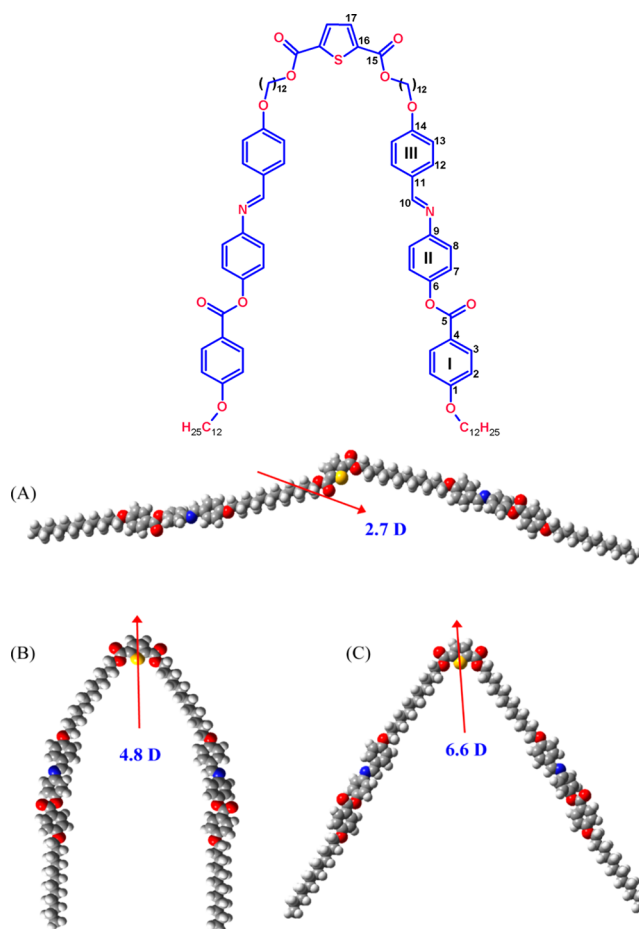


Figure 1. Molecular structure of mesogen S_{12} – C_{12} . Energy optimized space-filled models, magnitude, and direction of dipole moment (DFT) for different conformations: (A) linear shape, (B) U-shape and (C) V-shape.

(Figure 1B) has the side arm cores parallel to each other and to the C_{2v} axis, which is the polar axis of the molecule. A V-shaped conformation (Figure 1C) may also be envisaged where the side arm cores make an angle with respect to the C_{2v} axis as in the case of banana-like molecules. It may be expected that the gross shapes of these three extreme conformations would result in different molecular packing leading to different mesophase morphologies. The investigations presented here are aimed at understanding the observed mesophase properties in terms of the molecular shape and molecular organization.

Mesophase Transitions and Their Trends. The complete details of HOPM and DSC investigations for all the compounds are available in the [Supporting Information](#) (Figures S1–S3, Table S1). Only important aspects of these results are highlighted in this section. The HOPM studies revealed for the whole series of mesogens, viz., S_4-C_2 to $S_{12}-C_{12}$, the existence of enantiotropic nematic phase, confirmed by the observation of birefringent droplets on cooling the isotropic phase.⁴⁰ Upon further cooling the nematic phase, the smectic C mesophase is observed for those molecules in which the spacer length and the length of the terminal chain are optimal. Thus, the appearance of the smectic C is first noticed in S_4-C_8 as a monotropic phase, while for the rest of the mesogens, i.e., C_{10} and C_{12} , it appeared enantiotropically. The smectic C phase is realized for all C_{10} and C_{12} mesogens. For lower homologues, the occurrence of smectic C is governed by the spacer length. The length of the chain versus the length of the spacer also influences the nature of molecular organization in the smectic phase, which is discussed elsewhere. The nematic–isotropic (N–I) transition temperatures of the mesogens showed a decreasing trend with the increase in the terminal chain length for a given spacer length (Figure S4 of [Supporting Information](#)). The nematic mesophase range also showed decreasing trend with increase in terminal chain length. Similar behavior is noticed across the series, where increase in spacer length resulted in decrease in nematic phase range. For the N–I transition, the ΔH values were in the range of 0.4–0.98 k cal/mol and showed an increasing trend with the increase in spacer length. Thermogravimetric analysis (TGA) of two mesogens (S_6-C_2 and S_8-C_2) (Figure S5 of [Supporting Information](#)) is carried out to find the initial decomposition temperature since the clearing temperatures of them are in the range of ~ 250 – 275 °C. The TGA analysis reveals that the initial decomposition temperature is above 300 °C, which is higher than the clearing temperatures.

The smectic mesophase range, on the other hand, revealed increasing tendency with increase in terminal chain length, within the series as well as across the series. These trends suggest the segregation of incompatible parts of the mesogens, i.e., segregation of flexible aliphatic chains and spacer from rigid aromatic parts leading to lamellar order typical of smectic phases.⁴¹ These observations are additionally confirmed by DSC, where each mesogen is subjected to two heating and cooling cycles (Table S2 of [Supporting Information](#)). For smectogens, the DSC scans showed two types of behavior. For a majority of mesogens, the transition enthalpy values associated with nematic to smectic phases are found to be ~ 0.14 to 0.49 k cal/mol, whereas for S_4-C_8 , S_4-C_{10} , S_4-C_{12} , S_6-C_{10} , S_6-C_{12} , and S_8-C_{12} , the values are found to be about 6 times higher (~ 1.0 – 3 k cal/mol). Such a large difference in transition enthalpies for nematic–smectic C transition encouraged us to examine the HOPM textures of smectic C mesophases more carefully. It was observed that for the mesogens with low transition enthalpy values, transformation from nematic to smectic C was preceded by transition bars resulting in the schlieren texture.⁴² The phase associated with such mesogens with low transition enthalpies are categorized as usual smectic C phases. For those mesogens in which the transition enthalpies are higher, on the other hand, the HOPM showed unusual textures (Figure 2), and the associated phase is considered as unusual smectic C phase. These two phases also revealed different XRD patterns, which are presented in the next section.

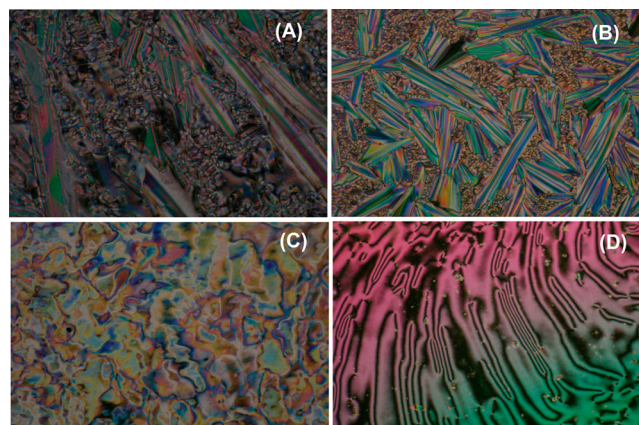


Figure 2. HOPM photographs of (A) S_4-C_{10} : 162.5 °C, (B) S_6-C_{12} : 142.2 °C (interdigitated partial bilayer smectic C phases), (C) $S_{12}-C_{12}$: 140 °C (monolayer smectic C phase) and (D) $S_{12}-C_{10}$: 186.2 °C (nematic phase).

The electric polarization studies of the mesogens exhibiting usual smectic mesophase as well as unusual smectic mesophase are carried out in respective mesophases. In both the cases, the polarization current peaks are not observed, even with the application of relatively high voltage, indicating the absence of layer polarization in these smectic phases.

Powder X-ray Diffraction Studies. The variable-temperature powder X-ray diffraction studies are undertaken to examine the molecular organization in the liquid crystalline phases and to obtain a correlation to the optical microscopy and scanning calorimetry results in terms of the molecular arrangement in the context of the appearance of usual and unusual smectic mesophases. Sixteen mesogens, some of which exhibit the usual and the others the unusual smectic mesophases, are examined by powder X-ray diffraction. XRD scans in the smectic C phase of two representative mesogens, namely S_6-C_8 and S_6-C_{10} are considered (Figure 3). For S_6-C_8 at 125 °C, the XRD shows a sharp peak at 30.87 Å in the small angle region and a broad diffuse peak at 4.44 Å in the wide angle region. The presence of the sharp reflection in the small angle region and a broad hump in the wide angle region suggests fluid lamellar ordering in the smectic mesophase⁴³ with layer spacing (d) equal to 30.87 Å. In contrast, for the other mesogen, namely, S_6-C_{10} , at 150 °C, three reflection peaks at 62.33, 31.13, and 20.67 Å are seen in the small angle region in addition to a broad diffuse peak at 4.47 Å in the wide angle region. The small angle reflections are indexed as (01), (02), and (03) planes of the lamellar structure with layer spacing as 62.33 Å. The broad hump in the wide angle region indicates liquid-like order within the layers. The higher orders of reflections suggest greater positional order in the smectic phases.⁴³ It is interesting to note that the layer spacing for S_6-C_{10} mesogen is approximately 2 times larger in comparison to that of S_6-C_8 . This remarkable increase in the layer spacing for a nominal increase in the terminal chain length indicates a different kind of molecular packing for the S_6-C_{10} homologue. Following this observation, the XRD data of all other mesogens are also examined. Typical values of reflections obtained for each of the 16 mesogens considered are listed in Table 1. The complete data obtained for all the mesogens at several temperatures are given in Table S3 of the [Supporting Information](#). Table 1 also shows the d/L ratio, where L is the molecular length. The value of L has been obtained by

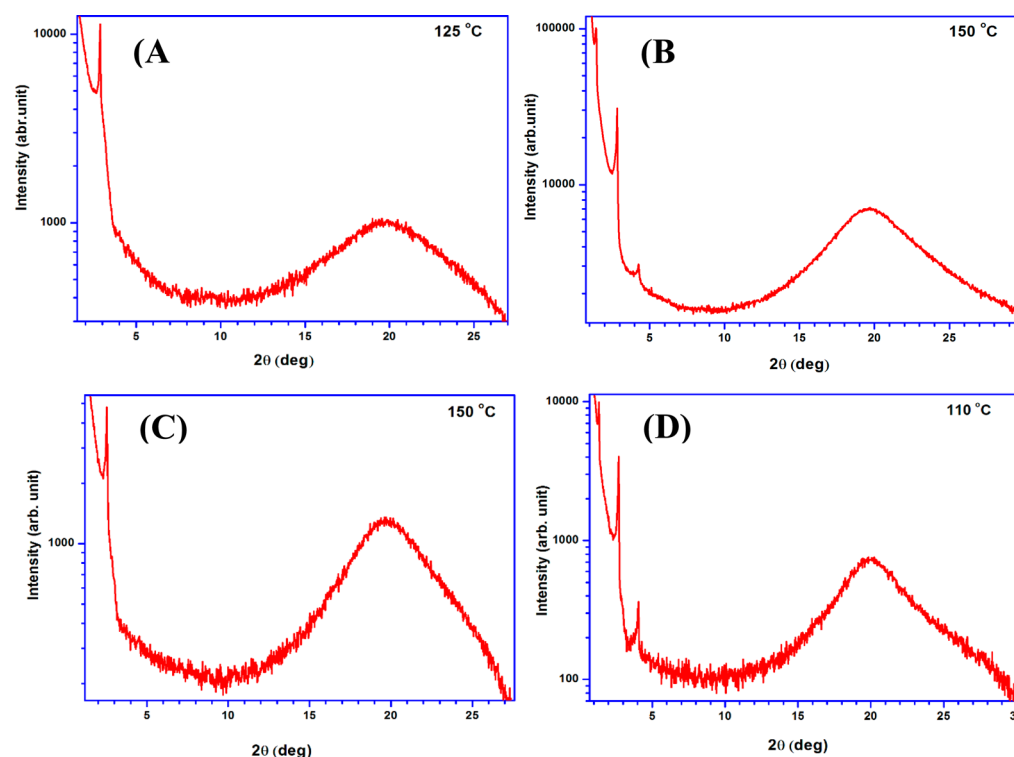


Figure 3. High-resolution X-ray powder diffraction patterns for (A) S_6-C_8 (125 °C), (B) S_6-C_{10} (150 °C), (C) S_8-C_{10} (150 °C), and (D) S_8-C_{10} (110 °C).

Table 1. Powder X-ray Diffraction Data of Mesogens at Representative Temperatures

| code | T (°C) | d_1 (Å) | d_2 (Å) | d_3 (Å) | d_4 (Å) | d/L |
|-----------------|----------|-----------|-----------|-----------|-----------|-------|
| S_4-C_{10} | 155 | 56.11 | 28.48 | 18.9 | 4.50 | 1.33 |
| S_4-C_{12} | 165 | 60.13 | 31.13 | - | 4.54 | 1.35 |
| S_6-C_8 | 125 | 30.87 | - | - | 4.44 | 0.73 |
| S_6-C_{10} | 140 | 61.22 | 30.58 | 20.38 | 4.44 | 1.37 |
| S_6-C_{12} | 145 | 63.55 | 32.35 | 21.64 | 4.53 | 1.39 |
| S_8-C_8 | 125 | 32.35 | - | - | 4.44 | 0.74 |
| S_8-C_{10} | 150 | 34.68 | - | - | 4.51 | 0.73 |
| | 110 | 66.05 | 32.67 | 21.70 | 4.46 | 1.42 |
| S_8-C_{12} | 135 | 68.04 | 34.31 | 22.87 | 4.49 | 1.42 |
| $S_{10}-C_6$ | 120 | 34.67 | - | - | 4.48 | 0.76 |
| $S_{10}-C_8$ | 130 | 35.05 | - | - | 4.44 | 0.75 |
| $S_{10}-C_{10}$ | 135 | 36.18 | - | - | 4.51 | 0.73 |
| $S_{10}-C_{12}$ | 130 | 37.31 | - | - | 4.43 | 0.72 |
| $S_{12}-C_6$ | 125 | 37.80 | - | - | 4.48 | 0.81 |
| $S_{12}-C_8$ | 130 | 38.24 | - | - | 4.47 | 0.77 |
| $S_{12}-C_{10}$ | 130 | 38.68 | - | - | 4.51 | 0.74 |
| $S_{12}-C_{12}$ | 140 | 40.06 | - | - | 4.52 | 0.74 |

tentatively assuming the U-like shape for the mesogens and calculating the L value by taking the length of the side arm core, the terminal chain, and the spacer lengths along with the thiophene unit, all of which are obtained from DFT calculations. For example, for the longest mesogen, namely, $S_{12}-C_{12}$, L is found to be 54 Å. For other mesogens, L varies in the range of 41.9–51.5 Å. From Table 1, it is noticed that in all the cases the wide angle peak occurs at nearly the same place (~ 4.5 Å). As seen in Figure 3 this peak is also a broad hump, indicating the fluid nature of the smectic phases.⁴⁴ The interesting features observed in the small angle region as well as the examination of data from Table 1, two kinds of behavior are

clearly noticed. The mesogens that exhibit the usual smectic phases show only one order of reflection in this region, similar to S_6-C_8 discussed earlier. The d/L ratios for these mesogens are in the range of 0.74–0.76. On the other hand, mesogens that display the unusual smectic phase show three orders of reflections as observed for the case of S_6-C_{10} . The d/L ratios in these cases are also different and occur in the range of 1.4–1.6. These observations suggest that the molecular packing for the usual and the unusual mesophases are not the same. This information correlates well with the different values of transition enthalpies for the two types determined from DSC measurements as well as with the differences in the HOPM textures mentioned earlier. In summary, the phases associated with the usual smectic C textures observed in HOPM have lower transition enthalpies for the nematic–smectic C (N–S) transition and have a smaller layer spacing of 34–40 Å as revealed by XRD. On the other hand, the phases associated with the unusual smectic C textures have higher transition enthalpies and have a larger layer spacing on the order of 56–70 Å.

It is of particular interest to note the XRD pattern of the S_8-C_{10} mesogen for which two significantly different layer spacings are noticed at different temperatures (Table 1). At 150 °C, the XRD scan shows a sharp reflection in the small angle region and a broad peak in the wide angle region. The corresponding layer spacing is 34.7 Å. At 110 °C, on the other hand, XRD shows three orders of reflection in the small angle region and a broad peak in the wide angle region. The layer spacing for this lower temperature phase is found to be 66.0 Å. The ratio of the layer spacing at the lower to the one at the higher temperature is about 1.9. Thus, lowering the temperature leads to a remarkable change in the molecular packing in the smectic phase of this particular mesogen. As discussed elsewhere, for this mesogen, the lengths of the terminal chain and the spacer

lie at the boundary where this series of mesogens make a transition from the usual to the unusual smectic phase, resulting in both the behaviors being observed. In this scenario, it would be interesting to investigate these mesogens using the solid state NMR methodology. As NMR provides information at the molecular level, it would be useful to know the molecular orientation and order as well as how the molecular subgroups are organized with respect to each other. Further differences in the molecular structures, if present in the different phases, will throw light on the origin of the phase behaviors. With this objective, NMR studies on two representative mesogens have been carried out, and the results are presented and discussed in the next section.

High-Resolution Solid State ^{13}C NMR Investigation.

^{13}C NMR measurements have been carried out on two representative mesogens, namely, $\text{S}_{12}\text{-C}_{12}$ and $\text{S}_6\text{-C}_{10}$. $\text{S}_{12}\text{-C}_{12}$ displays the usual smectic C phase, while the $\text{S}_6\text{-C}_{10}$ shows the unusual smectic C mesophase. The ^{13}C NMR spectrum of $\text{S}_{12}\text{-C}_{12}$ is considered for detailed discussion. Figure 4A shows the

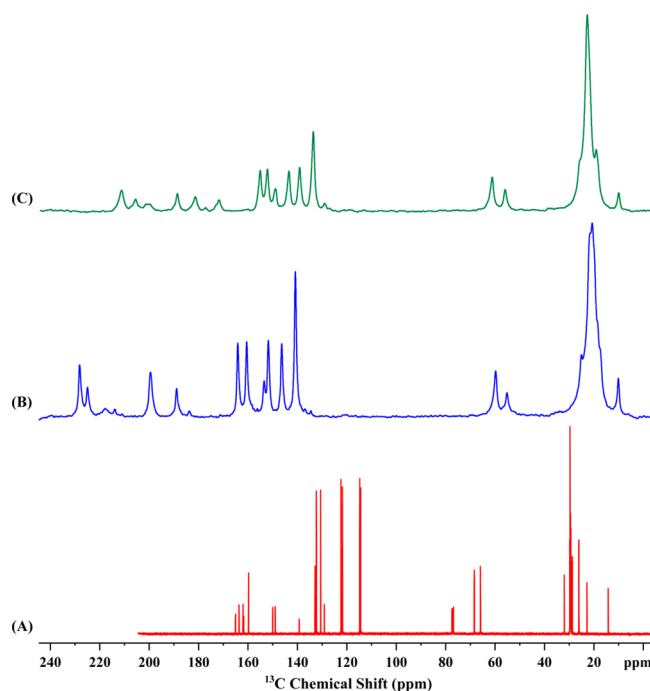


Figure 4. ^{13}C NMR spectra of $\text{S}_{12}\text{-C}_{12}$ in (A) solution, (B) smectic C phase (140 °C), and (C) nematic phase (175 °C).

proton decoupled ^{13}C NMR spectrum of the compound in solution. The assignment of these peaks is carried out by ACD chemsketch software, which is further refined by computing the chemical shifts by DFT calculations (Table 2). The appearance of only half the number of spectral lines in comparison to the total number of carbon atoms, particularly in the aromatic region where the chemical shift dispersion is high, suggests that both arms are chemically equivalent. For the case of the $\text{S}_6\text{-C}_{10}$ mesogen, the spectral features are similar to $\text{S}_{12}\text{-C}_{12}$ mesogen except for the difference in the number of signals in the aliphatic region due to the shorter spacer as well as the terminal chain lengths.

The spectrum of a static sample of the liquid crystal $\text{S}_{12}\text{-C}_{12}$ obtained in its smectic C and nematic phases are shown respectively in Figures 4B,C. These two spectra show a large dispersion in chemical shifts compared to the spectrum in the

isotropic phase, particularly in the aromatic region, due to the effect of chemical shift anisotropy coming into play in the liquid crystalline phase. The assignment of the spectra in the LC phase is carried out by comparing structurally similar fragments of mesogens, which are known from the literature.^{44,45} Information from the 2D-SLF spectra is also useful, which is discussed subsequently. Accordingly, the peaks appearing in the range 140–229 ppm are assigned to thiophene, linking units, and side arm phenyl ring carbons. The five peaks appearing in the region of 140–165 ppm in the smectic C phase have been assigned to the phenyl ring methine carbons with the intense peak at 140.7 ppm being assigned to two of them. The weak peak in this region at 153.4 ppm has assigned to the methine carbon (C_{17}) of thiophene. The identification of the characteristic imine carbon (C_{10}) signal at 199.6 ppm is enabled due to observation of a high $^{13}\text{C}\text{-}^1\text{H}$ dipolar coupling in the 2D spectrum. The spacer as well as the terminal chain carbon signals appears in the range 17–60 ppm. Similar observations for the spectra in the nematic phase (Figure 4C) have been made. Table 2 lists the assignment of the core as well as the thiophene carbons at two temperatures in the smectic phase and also at 175 °C in the nematic phase. The alignment-induced chemical shifts (AIS) are calculated as $\delta_{\text{LC}} - \delta_{\text{solution}}$ and are also listed in Table 2. The AIS suggests a parallel alignment of the side arm core unit in the magnetic field (Figure 5A). The observation of only one set of signals for both arms means that both the arms have identical orientation and order in the LC phase. For $\text{S}_6\text{-C}_{10}$ mesogen similar observations can also be made based on the spectra obtained in its smectic phase (Figure S6 of the Supporting Information).

Figure 5B shows the expanded 2D SLF spectrum of the side arm core and thiophene methine carbons of $\text{S}_{12}\text{-C}_{12}$ in the smectic C phase at 140 °C, while the full spectrum is shown in Figure S7 of Supporting Information. The 2D spectrum shows well-resolved contours arising from side arm core as well as spacer and terminal chain carbons. In the region of 140–229 ppm, the imine carbon contours (marked in green) and the thiophene methine carbon contours (marked in red) are clearly separated from the contours of the phenyl ring carbons. Table 2 lists the $^{13}\text{C}\text{-}^1\text{H}$ dipolar frequencies measured from 2D spectrum.

Figure 5C shows the expanded part of 2D spectrum depicting the side arm core and thiophene methine carbons of $\text{S}_{12}\text{-C}_{12}$ in the nematic phase at 175 °C. The trends noticed in the smectic C phase are also found in the nematic phase. Decrease in chemical shift as well as $^{13}\text{C}\text{-}^1\text{H}$ dipolar coupling values noticed in this phase are the result of the reduction in the orientational order parameters. The $^{13}\text{C}\text{-}^1\text{H}$ dipolar coupling values (Table 2) of phenyl ring methine carbons of the side arm core are comparable with those mesogens in which the core is constructed with three phenyl rings.^{44,45} The 2D-SLF experiments were also carried out in the smectic C and the nematic phases of $\text{S}_6\text{-C}_{10}$ mesogen, and the $^{13}\text{C}\text{-}^1\text{H}$ dipolar couplings are obtained, the details of which are available in the Supporting Information (Figure S8 and Table S4).

The local orientational order parameters of the phenyl rings of the mesogen $\text{S}_{12}\text{-C}_{12}$ have been calculated in its smectic and nematic mesophases from the experimental dipolar oscillation frequencies obtained from the 2D SLF technique by using the following equation:^{44–47}

Table 2. ^{13}C NMR Data of $\text{S}_{12}\text{-C}_{12}$ Mesogen in Solution and Liquid Crystalline Phases

| C. No | solution (ppm) | DFT (ppm) | smectic C 140 °C | | | smectic C 160 °C | | | nematic 175 °C | | |
|-------|----------------|-----------|------------------|-----------|----------|------------------|-----------|----------|----------------|-----------|----------|
| | | | CS (ppm) | AIS (ppm) | DC (kHz) | CS (ppm) | AIS (ppm) | DC (kHz) | CS (ppm) | AIS (ppm) | DC (kHz) |
| 1 | 161.9 | 163.6 | 228.0 | 66.1 | 1.62 | 220.0 | 58.1 | 1.36 | 211.7 | 49.8 | 1.13 |
| 2 | 114.2 | 114.2 | 140.7 | 26.5 | 2.95 | 137.4 | 23.2 | 2.56 | 134.1 | 19.9 | 2.20 |
| 3 | 132.2 | 134.0 | 160.4 | 28.2 | 2.97 | 156.5 | 24.3 | 2.60 | 152.7 | 20.5 | 2.26 |
| 4 | 121.6 | 121.9 | 188.8 | 67.2 | 1.60 | 180.7 | 59.1 | 1.31 | 172.5 | 50.9 | 1.11 |
| 5 | 164.9 | 164.6 | 214.0 | 49.1 | - | 206.9 | 42.0 | - | 200.1 | 35.2 | - |
| 6 | 148.9 | 149.4 | 224.9 | 76.0 | 1.68 | 215.6 | 66.7 | 1.42 | 206.1 | 57.2 | 1.17 |
| 7 | 121.6 | 120.6 | 146.2 | 24.6 | 3.20 | 142.9 | 21.3 | 2.76 | 139.7 | 18.1 | 2.39 |
| 8 | 122.2 | 124.3 | 151.7 | 29.5 | 2.97 | 147.9 | 25.7 | 2.63 | 144.1 | 21.9 | 2.30 |
| 9 | 149.9 | 149.2 | 228.0 | 78.1 | 1.62 | 220.0 | 70.1 | 1.36 | 211.7 | 61.8 | 1.13 |
| 10 | 159.6 | 153.9 | 199.6 | 40.0 | 5.00 | 194.6 | 35.0 | 4.38 | 189.4 | 29.8 | 3.78 |
| 11 | 129.0 | 131.4 | 199.6 | 70.6 | 2.18 | 190.7 | 61.7 | 1.83 | 182.0 | 53.0 | 1.52 |
| 12 | 130.4 | 132.7 | 163.9 | 33.5 | 2.78 | 159.8 | 29.4 | 2.48 | 155.7 | 25.3 | 2.12 |
| 13 | 114.6 | 117.9 | 140.7 | 26.1 | 2.95 | 137.4 | 22.8 | 2.56 | 134.1 | 19.5 | 2.20 |
| 14 | 161.6 | 161.6 | 228.0 | 66.4 | 1.62 | 220.0 | 58.4 | 1.36 | 211.7 | 50.1 | 1.13 |
| 15 | 163.5 | 159.8 | 214.0 | 50.5 | - | 206.9 | 43.4 | - | 200.1 | 36.6 | - |
| 16 | 139.1 | 143.6 | 183.8 | 44.7 | 0.81 | 181.1 | 42.0 | 0.56 | 177.7 | 38.6 | 0.51 |
| 17 | 132.7 | 131.8 | 153.4 | 20.7 | 1.67 | 151.9 | 19.2 | 1.50 | 149.4 | 16.7 | 1.31 |

CS: Chemical Shift; AIS: Alignment Induced Shift; DC: $^{13}\text{C}\text{-}^1\text{H}$ Dipolar Couplings

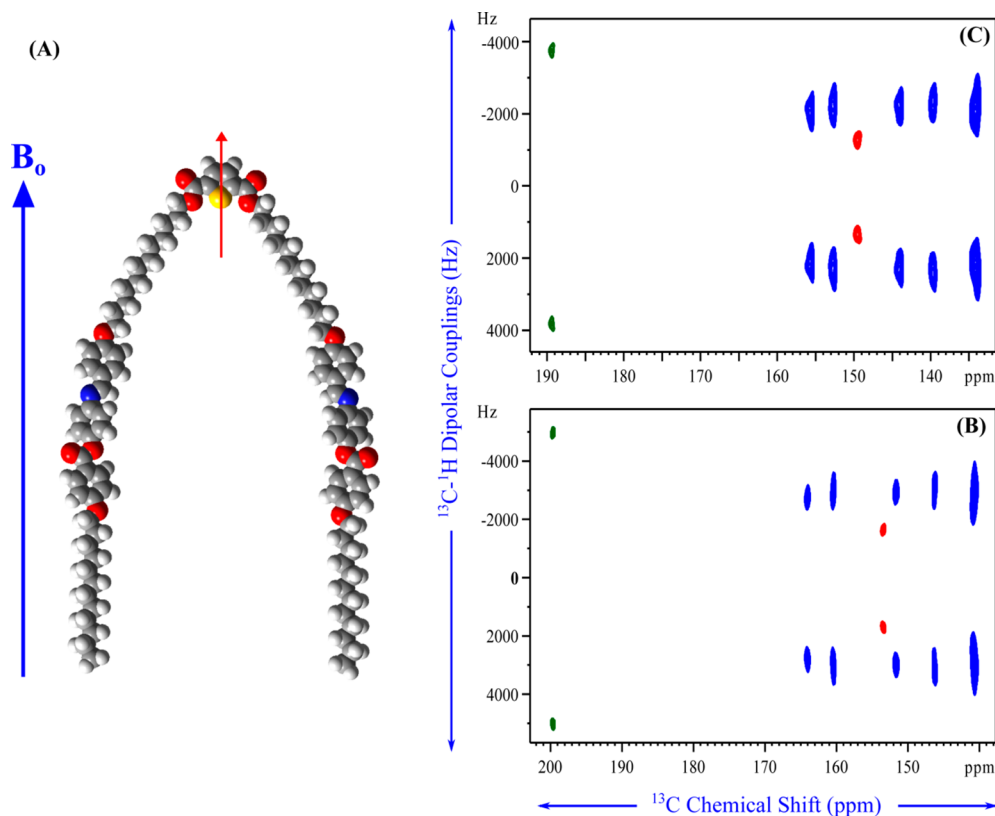
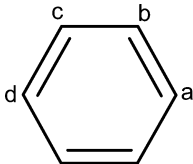


Figure 5. (A) Picture shows the orienting axis (C_{2v}) of $\text{S}_{12}\text{-C}_{12}$ mesogen, which is parallel to the magnetic field. 2D SAMPI-4 spectra of $\text{S}_{12}\text{-C}_{12}$ mesogen in (B) smectic C phase at 140 °C and (C) nematic phase at 175 °C. Red and green contours denote thiophene ring methine and imine carbons.

$$D_{\text{CH}} = K \left[\frac{1}{2} (3 \cos^2 \theta_z - 1) S'_{zz} + \frac{1}{2} (\cos^2 \theta_x - \cos^2 \theta_y) (S'_{xx} - S'_{yy}) \right] \quad (1)$$

where $K = -h\gamma_{\text{H}}\gamma_{\text{C}}/4\pi^2 r_{\text{CH}}^3$, γ_{H} and γ_{C} are the gyromagnetic ratios of ^1H and ^{13}C nuclei, respectively, and θ_x , θ_y , and θ_z are angles between the internuclear vector, r_{CH} , and the coordinate axes. For the phenyl rings, the z -axis is taken as the para-axis

(C_2 axis) of the ring; the x -axis is in the plane of the ring, while the y -axis is perpendicular to the plane. Standard bond distances, namely 1.1 Å for the C–H bond and 1.4 Å for the C–C bond, are taken for calculating K in eq 1. By following the established procedure,^{38,39,44–48} the two order parameters, namely, S'_{zz} and $(S'_{xx} - S'_{yy})$ for the phenyl rings, are calculated by using eq 1. The estimated orientational order parameter values for phenyl rings in the smectic C and nematic phases are

Table 3. Orientational Order Parameter Values of Phenyl Rings^a and the Thiophene Ring of S₁₂–C₁₂ Mesogen


| ring | T (°C) | angles | | S'_{zz} | $S'_{xx} - S'_{yy}$ | calculated dipolar oscillation frequencies (kHz) | | | |
|------|--------|------------|------------|-----------|---------------------|--|------|----------------|------|
| | | θ_b | θ_c | | | b | c | a ^b | d |
| I | 140 | 120.1 | 120.0 | 0.69 | 0.076 | 2.95 | 2.98 | 1.61 | 1.60 |
| II | | 119.7 | 120.3 | 0.71 | 0.080 | 3.18 | 2.98 | 1.65 | 1.66 |
| III | | 120.7 | 120.1 | 0.69 | 0.078 | 2.77 | 2.96 | 2.18 | 1.61 |
| I | 160 | 119.9 | 119.7 | 0.58 | 0.066 | 2.55 | 2.60 | 1.35 | 1.34 |
| II | | 119.5 | 120.0 | 0.60 | 0.071 | 2.77 | 2.63 | 1.39 | 1.40 |
| III | | 120.2 | 119.9 | 0.58 | 0.068 | 2.48 | 2.56 | 1.83 | 1.35 |
| I | 175 | 119.6 | 119.3 | 0.49 | 0.052 | 2.20 | 2.26 | 1.13 | 1.12 |
| II | | 119.2 | 119.5 | 0.50 | 0.060 | 2.39 | 2.32 | 1.16 | 1.16 |
| III | | 120.0 | 119.6 | 0.49 | 0.053 | 2.11 | 2.20 | 1.54 | 1.13 |

| thiophene | T (°C) | tilt angle θ | S'_{zz} | $S'_{xx} - S'_{yy}$ | calculated dipolar oscillation frequencies (kHz) | |
|-----------|--------|---------------------|-----------|---------------------|--|------|
| | | | | | C17 | C16 |
| | 140 | 34.0 | 0.41 | 0.158 | 1.67 | 0.73 |
| | 160 | 29.0 | 0.25 | 0.043 | 1.50 | 0.50 |
| | 175 | 30.0 | 0.23 | 0.036 | 1.31 | 0.44 |

^aIn the figure above the table, b and c are methine carbons, and a and d are quaternary carbons, respectively, for rings I, II, and III. ^bFor carbon a in ring-III, the contribution of the azomethine proton has also been taken into account.

shown in Table 3. The order parameter of the side arm core is taken to be the same as that of the phenyl ring-II, which is more ordered than ring-I and ring-III. Accordingly, the S_{zz} values are found to respectively be 0.71 and 0.60 at 140 and 160 °C in the smectic phase and 0.50 at 175 °C in the nematic phase. For the S₆–C₁₀ mesogen, these values are 0.69 at 140 °C in the smectic C and 0.64 at 160 °C in the nematic phase (Table S5 of the Supporting Information). These values are consistent with typical mesogens constructed with three phenyl rings for which literature data is available.^{44,45}

The order parameters of the center thiophene ring have been obtained from the experimental ¹³C–¹H dipolar oscillation frequencies of the thiophene carbons using a model in which the plane of the thiophene ring is oriented at an angle with respect to the C_{2v} axis of the molecule, which is aligned with the magnetic field (Figures S5A and S9 of the Supporting Information). Values of 0.41, 0.25, and 0.23 for S'_{zz} , respectively, at 140, 160, and 175 °C are obtained for the thiophene moiety of the S₁₂–C₁₂ mesogen (Table 3). For S₆–C₁₀ the corresponding values are 0.23 and 0.19, respectively, at 140 and 160 °C phase (Table S6 of the Supporting Information). The low S'_{zz} value for thiophene in comparison to the side arm phenyl rings is due to the presence of the flexible spacer between the thiophene and the side arm core resulting in the increased mobility of the thiophene ring. In Table 3 it is seen that, with the increase in temperature, the order parameters decrease as the phase changes from smectic C to nematic. The ¹³C NMR measurements of the mesogens in the smectic C as well as in the nematic phases indicate that the C_{2v} symmetry axis of the molecule is parallel to the magnetic field (Figure S5A). The results are also taken to support the hypothesis that the molecule adopts a U-shape rather than a V-shape. This is based on the argument that for a V conformation, the central thiophene and the attached spacers will be rigid, and the thiophene ring will have an order parameter comparable to

or higher than the side arm phenyl rings. In such a case, as obtained with other bent-core systems,^{38,39} the bent-angle β can be calculated from $S'_{zz}(\text{Phe}_{\text{II}}) = P_2 \cos(\beta) \cdot S'_{zz}(\text{Thio})$, where $S'_{zz}(\text{Phe}_{\text{II}})$ and $S'_{zz}(\text{Thio})$ are the order parameters of the side arm phenyl ring-II and the thiophene ring, respectively. However, a lower order parameter for the thiophene ring as well as the local order parameter of the attached O–CH₂ carbons indicates that this part of the molecule is relatively flexible and cannot support a V-shape. Thus, NMR measurements of both types of molecules, namely those which exhibit the usual smectic C phase as exemplified by S₁₂–C₁₂ and those which exhibit the unusual smectic C phase similar to S₆–C₁₀, indicate the U-like conformation for both series. It may be noted that despite a large variation in d/L ratios between the two series of molecules arising out of the monolayer versus interdigitated bilayer smectic C organization, they have comparable orientational order parameter values, which suggests that the different molecular packing has no significant impact on the local molecular dynamics.

Model of Molecular Organisation. The set of mesogens investigated here, though they can be classified as symmetric dimers, are unusual for the reason that the two arms of the dimer are not joined by a simple aliphatic chain, but with a flexible spacer and a rigid thiophene unit at the center. For such a configuration, three major possible shapes as depicted in Figure 1 are possible. Among these, for the linear conformation (Figure 1A), the L value is nearly double that of the other two. The conventional linear symmetrical dimers are in general observed to exhibit intercalated phases with a typical d/L ratio of 0.5.^{1–7} This is, however, not considered as a possibility in our case, as the central thiophene dicarboxylate unit is expected to promote for the molecule a bent shape rather than a linear shape for the reason that the bend angle of 2,5-thiophene dicarboxylate is typically 145°. ⁴⁹ It was shown previously³⁸ that, without the flexible spacer and only with a thiophene unit

connecting the two arms, the molecule can be classified as a bent core mesogen and has a V shape. The molecule orients in the magnetic field with the C_{2v} symmetry axis of the molecule perpendicular to the magnetic field. The thiophene moiety is rigid and shows a large order parameter. However, in the present case, we rule out the V-shape conformation shown in Figure 1C, as the mesophases observed are different from the smectic phases exhibited by the bent core banana like molecules.⁵⁰ The switching current experiments confirmed the absence of layer polarization in these smectic phases. Further, the layer ordering as well as layer spacing does not support the V-shape. With the flexible spacer unit connecting the thiophene to the side arm core units, the NMR results support a U shape for the molecule, since it is observed that the thiophene unit is much less rigid and has a relatively lower order parameter. The molecule also orients with the C_{2v} symmetry axis parallel to the magnetic field. Based on these observations, it is concluded that the molecule most probably adopts the U-shaped conformation, as shown in Figure 1B.

In this series of mesogens, molecules exhibit a variety of phases depending on the length of the spacer unit and the terminal chain length. These are summarized in Figure 6A. As

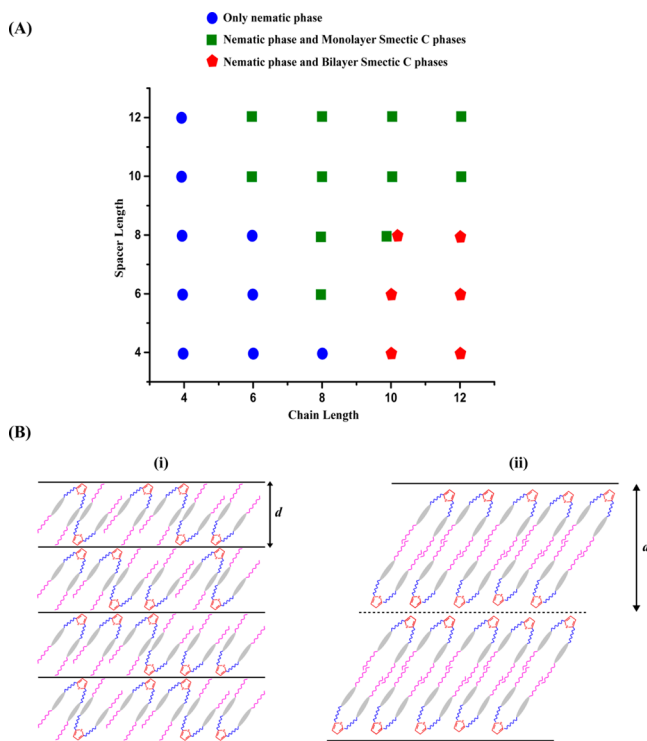


Figure 6. (A) The phase characteristics of mesogens as a function of spacer and terminal chain length. (B) Schematic representation of (i) usual smectics, tilted monolayer organization, and (ii) unusual smectics, tilted interdigitated partial bilayer organization.

seen in the figure, molecules with shorter spacer and terminal chain lengths exhibit only the nematic phase, while those with more numbers of carbons either in the spacer unit or in the terminal chain exhibit the smectic phase also. In the smectic phase, two different types are observed, which have been named as the usual and the unusual smectic phases. The distinction between the usual and the unusual smectic phases has been made based on HOPM, DSC, and XRD results. The XRD results reveal for the usual smectic C phases a smaller

layer spacing of 34–40 Å, while for the unusual phases larger layer spacing on the order of 56–70 Å is observed. With the assumption of a U shape for the molecules, the molecular length L has been calculated, and this gives rise to a d/L ratio in the range of 0.74–0.76 for the smectic C phase. This corresponds to a tilted monolayer organization of the U-shaped molecules in the layers is proposed. The tilt angle θ determined from the d/L ratio is found to be about 40° , which agrees with that estimated from the HOPM studies. On the other hand, for the unusual smectic mesophases, a tilted interdigitated partial bilayer organization⁵¹ of the U-shaped molecules is considered, which accounts for the d/L ratio being greater than 1 but less than 2. The dipole moment values of the three shapes presented in Figure 1 calculated from DFT are 2.7, 4.8, and 6.6 D for the linear, U-shaped, and V-shaped molecules, respectively. The large longitudinal dipole moment of the thiophene unit in the U-shaped configuration tends to stabilize the interdigitated partial bilayer organization of the molecules in layers. It is known in the literature that highly polar group attached to one end of a rigid rod-like molecules often leads to such interdigitated partial bilayer organization and double-layer arrangements of the molecules in layers.⁵² It is interesting to note that a highly polar group such as the cyano group, even if it is only attached to one end of the rigid core through a flexible aliphatic spacer chain, leads to the formation of a double-layered SmA_2 phase.⁵³ The strong dipolar interaction of the highly polar end groups tends to stabilize these higher order smectic phases, even when the polar end group is mechanically decoupled from the rigid core through a flexible aliphatic chain.

Based on the above observations, a model for the molecular packing for both types of smectic phases is shown in Figure 6B. For the usual smectics, the tilted monolayer organization is suggested (Figure 6B(i)) that takes into account the observed d/L ratio of 0.74 and the tilt angle of 40° for the molecules within the layer. Similarly, for the unusual smectics, the tilted interdigitated partial bilayer structure is shown in Figure 6B(ii), which corresponds to a larger d/L ratio of 1.4. In order to understand the driving force responsible for the two dissimilar molecular packing for the synthesized mesogens, it would be useful to consider the existing information for dimers/trimers reported in the literature. For instance, malonic acid-based⁵⁴ dimers revealed the presence of nematic and smectic A phases with a typical layer intercalation. The replacement of malonic acid in these mesogens with thiophene dicarboxylate yields the present mesogens. From this it is easy to recognize the role of thiophene in influencing the phase properties. Similarly, mesogens with a three ring core linked to a hydroxyl alkoxy chain at one end and an alkoxy chain at the other end⁴⁴ show an enantiotropic nematic and the usual smectic C phases similar to the thiophene mesogens. This observation indicates that the side arms also play a part in deciding the phase characteristics of the current set of mesogens. These are further illustrated in Figure 6A, which shows the various phases exhibited by the current set of mesogens as a function of the number of carbon atoms in the spacer unit and the terminal chain. In the figure, it may be noticed that, for shorter spacer and terminal chains, only nematic phases are noticed. With increasing length of either the spacer unit or the terminal chain, the smectic phases start appearing. It may be noted that increasing the terminal chain length favors the formation of the unusual smectic phase (interdigitated partial bilayer configuration), while increasing the spacer length favors the formation of the usual smectic

phase (monolayer configuration). For example, in the case of the C-12 mesogens, for shorter spacer lengths, namely, S-4, S-6, and S-8, the bilayer smectics are observed, while for S-10 and S-12 the monolayer smectics are seen. Interestingly, the S₈–C₁₀ mesogen lies at the crossing point of these two behaviors, and for this case both phases are observed as a function of temperature. The transition is found to be weakly first-order with the bilayer conformation being favored at the lower temperature. It may be mentioned that a similar behavior has been postulated in side-chain liquid crystalline polymers where the mesogens are attached to the main chain through a flexible spacer, with the short spacer favoring the bilayer formation, while the longer ones result in monolayer organization.^{55,56} Another important result comes from the polarization measurements, which revealed that both the usual and unusual smectic mesophases are nonswitchable. Despite the polar nature of the mesogens, the absence of net-polarity signifies an antiparallel packing of the mesogens. Based on this fact and considering the effect of the longer terminal chains, one may conclude that the thiophene–thiophene interaction coupled with the interaction between the side-chains favors the bilayer configuration in mesogens with a short spacer. Increasing the length of the spacer or increasing temperature as in the case of S₈–C₁₀ mesogen gives rise to additional mobility at the thiophene end of the molecule, leading to collapse of the bilayer arrangement. Thus, the monolayer configuration is preferred for mesogens with a longer spacer length. These trends suggest that the driving force responsible for the formation of the molecular arrangements is the segregation of incompatible parts of the mesogens combined with steric frustration, leading to lamellar order.⁵⁷ Thus, the findings here provide an understanding of the properties of the mesogens investigated, which behave differently than classical dimers, and also of the role of the polar five membered thiophene ring at the middle in the mesogens in influencing these properties.

CONCLUSION

Thirty mesogens built with thiophene at the center and linked to a side-arm, three-phenyl ring core by flexible spacers as well as terminal alkoxy chains exhibited enantiotropic mesophases. The mesogens with short spacer and terminal chains showed predominantly nematic mesophase, while longer spacer and terminal chains favored both nematic and smectic C phases. The HOPM and DSC investigations revealed the following two kinds of smectic C mesophases: (i) a phase with typical schlieren textures and with normal enthalpy values and (ii) a phase with unusual textures associated with high transition enthalpy. A detailed XRD investigation of the mesogens in the smectic C phase revealed different features for the above two cases. The layer spacing and d/L ratio for mesogens exhibiting the unusual smectic C phase was found to be higher than those of mesogens exhibiting the usual smectic C phase. By considering the U-shape as the most preferred conformation, the molecular organization in the usual smectic C phase was found to be a monolayer, while for the unusual case an interdigitated partial bilayer organization has been suggested. Interestingly, for one of the homologues, S₈–C₁₀, both types of molecular organization are observed with a transition from monolayer to interdigitated partial bilayer smectic C mesophase taking place by a decrease of temperature. ¹³C NMR measurements carried out in the nematic and the smectic C mesophases of two of the mesogens showed that there is a large variation in the order parameters between the thiophene ring

and the side-arm phenyl rings. This arises because of the flexible spacer that connects the thiophene to the side-arm core phenyl rings. The results have been interpreted to indicate a U-shape conformation for the mesogens. The absence of net polarity as indicated by polarization measurements supports an antiparallel packing of the mesogens in the smectic C phase. A systematic analysis of the above results in terms of the length of the spacer versus the length of the chain has been made, and the results indicate that the spacer length plays an important role in influencing the molecular organization in terms of monolayer versus bilayer arrangement. It is, however, necessary to recognize the role of the other components of the molecule such as the thiophene moiety in influencing the molecular arrangements. The molecular shape, say U or V, may also be expected to significantly influence the property of the phase.

ASSOCIATED CONTENT

Supporting Information

The Supporting Information is available free of charge on the ACS Publications website at DOI: 10.1021/acs.langmuir.5b02327.

Synthetic details of 30 mesogens as well as experimental conditions employed for generating the data from different techniques. Further, tables and figures of DSC, a table of T/T_{N-SC} and d/L ratios, and figures of T_{N-I} versus terminal chain length, T_{N-I} versus spacer length, T_{SC-N} versus terminal chain length, HOPM images of the mesogens, SAMPI-4 pulse sequence, 1D as well as 2D static liquid crystalline ¹³C NMR plots and orientational order data of S₆–C₁₀ mesogen, a proposed model for the thiophene unit, and TGA curves for mesogens are also included. (PDF)

AUTHOR INFORMATION

Corresponding Author

*E-mail: kvr@sif.iisc.ernet.in.

Present Address

[†]Chemical Physics Laboratory, CSIR-Central Leather Research Institute, Adyar, Chennai, 600020, India.

Notes

The authors declare no competing financial interest.

ACKNOWLEDGMENTS

M.K.R. would like to thank Prof. K. Subramanyam Reddy, Sri Venkateswara University, Tirupati, India, and Dr. A. B. Mandal, CSIR-CLRI, Chennai, India, for their help, constant support, and encouragement. The authors are grateful to Prof. V. A. Raghunathan and Ms. K. N. Vasudha, RRI, Bangalore, India, for the X-ray measurements. Thanks are also due to Dr. V. Subramanian, CLRI, for the quantum chemical calculations. The partial financial support from STRAIT project under XII five year plan of CSIR is duly acknowledged. The use of the Bruker AV-III-400 and Bruker AV-III-500 WB NMR spectrometers funded by the Department of Science and Technology, New Delhi, at the NMR Research Centre, Indian Institute of Science, Bangalore, India, is gratefully acknowledged.

REFERENCES

- (1) Henderson, P. A.; Imrie, C. T. Methylene-Linked Liquid Crystal Dimers and the Twist-Bend Nematic Phase. *Liq. Cryst.* **2011**, *38*, 1407–1414.

- (2) Imrie, C. T.; Henderson, P. A. Liquid Crystal Dimers and Higher Oligomers: Between Monomers and Polymers. *Chem. Soc. Rev.* **2007**, *36*, 2096–2124.
- (3) Imrie, C. T.; Henderson, P. A. Liquid Crystal Dimers and Oligomers. *Curr. Opin. Colloid Interface Sci.* **2002**, *7*, 298–311.
- (4) Narumi, T.; Miura, Y.; Ashina, T.; Yoshizawa, A. Preorganised Effects of a Tetramesogenic Supermolecule on Supramolecular Assembly in the Liquid Crystalline Phases. *Liq. Cryst.* **2011**, *38*, 639–648.
- (5) Attard, G. S.; Garnett, S.; Hickman, C. G.; Imrie, C. T.; Taylor, L. Asymmetric Dimeric Liquid Crystals with Charge Transfer Groups. *Liq. Cryst.* **1990**, *7*, 495–508.
- (6) Faye, V.; Nguyen, H. T.; Barois, P. From Segregation to Intercalation in Smectic Organization of Polar Non-Symmetric Dimesogens. *J. Phys. II* **1997**, *7*, 1245–1260.
- (7) Yamaguchi, A.; Watanabe, M.; Yoshizawa, A. Odd-Even effects for Phase Transition Behaviour of Novel U-shaped Liquid Crystals. *Liq. Cryst.* **2007**, *34*, 633–639.
- (8) Shanavas, A.; Sathiyaraj, S.; Chandramohan, A.; Narasimhaswamy, T.; Sultan Nasar, A. Isophthalic Acid Based Mesogenic Dimers: Synthesis and Structural Effects on Mesophase Properties. *J. Mol. Struct.* **2013**, *1038*, 126–133.
- (9) Chan, T.-N.; Yeap, G.-Y.; Yam, W.-S.; Madrak, K.; Zep, A.; Pociecha, D.; Gorecka, E. A Crossover from Rod-Shaped to Bent-Shaped in Symmetric Isoflavone Liquid Crystal Trimers Exhibiting Unusual Mesomorphic Behaviour. *J. Mater. Chem.* **2012**, *22*, 11335–11339.
- (10) Yoshizawa, A.; Nakata, M.; Yamaguchi, A. Phase Transition Behaviour of Novel Y-shaped Liquid Crystal Oligomers. *Liq. Cryst.* **2006**, *33*, 605–609.
- (11) Yoshizawa, A.; Kinbara, H.; Narumi, T.; Yamaguchi, A.; Dewa, H. Synthesis and Physical Properties of Novel Liquid Crystal Trimers Possessing Resorcinol as a Linking Unit. *Liq. Cryst.* **2005**, *32*, 1175–1181.
- (12) Demus, D. One Hundred Years of Liquid-Crystal Chemistry: Thermotropic Liquid Crystals with Conventional and Unconventional Molecular Structure. *Liq. Cryst.* **1989**, *5*, 75–110.
- (13) Attard, G. S.; Douglass, A. G.; Imrie, C. T.; Taylor, L. Liquid-Crystalline Cyclic Trimers Derived from Benzene-1, 3, 5-tricarboxylic acid. *Liq. Cryst.* **1992**, *11*, 779–784.
- (14) Goring, P.; Pelzl, G.; Diele, S.; Delavier, P.; Siemensmeyer, K.; Etzbach, K. H. Phase Transitions Between Smectic A Phases as well as Smectic C* Phases and Undulated Structures in Terminal Non-Polar Compounds. *Liq. Cryst.* **1995**, *19*, 629–635.
- (15) Yamaguchi, A.; Nishiyama, I.; Yamamoto, J.; Yokoyama, H.; Yoshizawa, A. Unusual Smectic Phases Organized by Novel λ -shaped Mesogenic Molecules. *J. Mater. Chem.* **2005**, *15*, 280–288.
- (16) Kolpaczynska, M.; Madrak, K.; Mieczkowski, J.; Gorecka, E.; Pociecha, D. H-Shaped Liquid Crystalline Dimers. *Liq. Cryst.* **2011**, *38*, 149–154.
- (17) Bialecka-Florjanczyk, E.; Sledzinska, I.; Gorecka, E.; Przedmojski, J. Odd–Even Effect in Biphenyl-Based Symmetrical Dimers with Methylene Spacer—Evidence of the B₄ phase. *Liq. Cryst.* **2008**, *35*, 401–406.
- (18) Francescangeli, O.; Samulski, E. T. Insights into the Cybotactic Nematic Phase of Bent-Core Molecules. *Soft Matter* **2010**, *6*, 2413–2420.
- (19) O'Neill, M.; Kelly, S. M. Ordered Materials for Organic Electronics and Photonics. *Adv. Mater.* **2011**, *23*, 566–584.
- (20) Seed, A. J.; Cross, G. J.; Toyne, K. J.; Goodby, J. W. Novel, Highly Polarizable Thiophene Derivatives for Use in Nonlinear Optical Applications. *Liq. Cryst.* **2003**, *30*, 1089–1107.
- (21) Brown, J. W.; Byron, D. J.; Harwood, D. J.; Wilson, R. C.; Tajbakhsh, A. R. Some Three-Ring Esters Containing a Five-Membered Heteroaromatic Ring. A Comparison of Liquid Crystal Properties. *Mol. Cryst. Liq. Cryst.* **1989**, *173*, 121–140.
- (22) Madsen, L. A.; Dingemans, T. J.; Nakata, M.; Samulski, E. T. Thermotropic Biaxial Nematic Liquid Crystals. *Phys. Rev. Lett.* **2004**, *92*, 145505-1–145505-4.
- (23) Francescangeli, O.; Vita, F.; Ferrero, C.; Dingemans, T.; Samulski, E. T. Cybotaxis Dominates the Nematic Phase of Bent-Core Mesogens: A Small-Angle Diffuse X-Ray Diffraction Study. *Soft Matter* **2011**, *7*, 895–901.
- (24) Gortz, V.; Southern, C.; Roberts, N. W.; Gleeson, H. F.; Goodby, J. W. Unusual Properties of a Bent-Core Liquid-Crystalline Fluid. *Soft Matter* **2009**, *5*, 463–471.
- (25) Vita, F.; Placentino, I. F.; Ferrero, C.; Singh, G.; Samulski, E. T.; Francescangeli, O. Electric Field Effect on the Phase Diagram of a Bent-Core Liquid Crystal. *Soft Matter* **2013**, *9*, 6475–6481.
- (26) Muraoka, T.; Shima, T.; Hamada, T.; Morita, M.; Takagi, M.; Tabata, K. V.; Noji, H.; Kinbara, K. Ion Permeation by a Folded Multiblock Amphiphilic Oligomer Achieved by Hierarchical Construction of Self-Assembled Nanopores. *J. Am. Chem. Soc.* **2012**, *134*, 19788–19794.
- (27) Kim, H.-J.; Liu, F.; Ryu, J.-H.; Kang, S.-K.; Zeng, X.; Ungar, G.; Lee, J.-K.; Zin, W.-C.; Lee, M. Self-Organization of Bent Rod Molecules into Hexagonally-Ordered Vesicular Columns. *J. Am. Chem. Soc.* **2012**, *134*, 13871–13880.
- (28) Peterca, M.; Imam, M. R.; Leowanawat, P.; Rosen, B. M.; Wilson, D. A.; Wilson, C. J.; Zeng, X.; Ungar, G.; Heiney, P. A.; Percec, V. Self-Assembly of Hybrid Dendrons into Doubly Segregated Supramolecular Polyhedral Columns and Vesicles. *J. Am. Chem. Soc.* **2010**, *132*, 11288–11305.
- (29) Radhika, S.; Monika, M.; Sadashiva, B. K.; Roy, A. Novel Zigzag-Shaped Compounds Exhibiting Apolar Columnar Mesophases with Oblique and Rectangular Lattices. *Liq. Cryst.* **2013**, *40*, 1282–1295.
- (30) Becke, A. D. Density-Functional Thermochemistry. III. The Role of Exact Exchange. *J. Chem. Phys.* **1993**, *98*, 5648–5652.
- (31) Lee, C. T.; Yang, W. T.; Parr, R. G. Development of the Colle-Salvetti Correlation Energy Formula into a Functional of the Electron Density. *Phys. Rev. B: Condens. Matter Mater. Phys.* **1988**, *37*, 785–789.
- (32) Ditchfield, R. Molecular Orbital Theory of Magnetic Shielding and Magnetic Susceptibility. *J. Chem. Phys.* **1972**, *56*, 5688–5691.
- (33) Cheeseman, J. R.; Trucks, G. W.; Keith, T. A.; Frisch, M. J. A Comparison of Models for Calculating Nuclear Magnetic Resonance Shielding Tensors. *J. Chem. Phys.* **1996**, *104*, 5497–5509.
- (34) Aliev, A. E.; Courtier-Murias, D. C.; Zhou, S. Scaling Factors for Carbon NMR Chemical Shifts Obtained from DFT B3LYP Calculations. *J. Mol. Struct.: THEOCHEM* **2009**, *893*, 1–5.
- (35) Frisch, M. J.; Trucks, G. W.; Schlegel, H. B.; Scuseria, G. E.; Robb, M. A.; Cheeseman, J. R.; Scalmani, G.; Barone, V.; Mennucci, B.; Petersson, G. A. et al. *Gaussian 09*, revision A.02; Gaussian, Inc.: Wallingford, CT, 2009.
- (36) Fung, B. M.; Khitrin, A. K.; Ermolaev, K. An Improved Broad Band Decoupling Sequence for Liquid Crystals and Solids. *J. Magn. Reson.* **2000**, *142*, 97–101.
- (37) Nevzorov, A. A.; Opella, S. J. Selective Averaging for High Resolution Solid-State NMR Spectroscopy of Aligned Samples. *J. Magn. Reson.* **2007**, *185*, 59–70.
- (38) Kesava Reddy, M.; Varathan, E.; Lobo, N. P.; Das, B. B.; Narasimhaswamy, T.; Ramanathan, K. V. High-Resolution Solid State ¹³C NMR Studies of Bent-Core Mesogens of Benzene and Thiophene. *J. Phys. Chem. C* **2014**, *118*, 15044–15053.
- (39) Kesava Reddy, M.; Varathan, E.; Jacinth, B.; Lobo, N. P.; Roy, A.; Narasimhaswamy, T.; Ramanathan, K. V. Structural investigation of resorcinol based symmetrical banana mesogens by XRD, NMR and polarization measurements. *Phys. Chem. Chem. Phys.* **2015**, *17*, 5236–5247.
- (40) Dierking, I. *Textures of Liquid Crystals*; Wiley-VCH: Weinheim, Germany, 2003.
- (41) Goodby, J. W. In *Hand Book of Liquid Crystals*; Demus, D., Goodby, J. W., Gray, G. W., Spiess, H. W., Vill, V., Eds.; Wiley-VCH: Weinheim, Germany, 1998; Vol. 2A, pp 411–440.
- (42) Guillevis, M. A.; Light, M. E.; Coles, S. J.; Gelbrich, T.; Hursthouse, M. B.; Bruce, D. W. Synthesis of Dinuclear Complexes of Rhenium(I) as Potential Metallomesogens. *J. Chem. Soc., Dalton Trans.* **2000**, *9*, 1437–1445.

- (43) Seddon, J. M. In *Hand Book of Liquid Crystals* Demus, D., Goodby, J. W., Gray, G. W., Spiess, H. W., Vill, V., Eds.; Wiley-VCH: Weinheim, Germany, 1998; Vol. 1, pp 635–679.
- (44) Kalaivani, S.; Narasimhaswamy, T.; Das, B. B.; Lobo, N. P.; Ramanathan, K. V. Phase Characterization and Study of Molecular Order of a Three-Ring Mesogen by ^{13}C NMR in Smectic C and Nematic Phases. *J. Phys. Chem. B* **2011**, *115*, 11554–11565.
- (45) Domenici, V.; Lelli, M.; Cifelli, M.; Hamplova, V.; Marchetti, A.; Veracini, C. A. Conformational Properties and Orientational Order of a De Vries Liquid Crystal Investigated through NMR Spectroscopy. *ChemPhysChem* **2014**, *15*, 1485–1495.
- (46) Xu, J.; Fodor-Csorba, K.; Dong, R. Y. Orientational Ordering of a Bent-Core Mesogen by Two-Dimensional ^{13}C NMR Spectroscopy. *J. Phys. Chem. A* **2005**, *109*, 1998–2005.
- (47) Fung, B. M.; Afzal, J.; Foss, T. L.; Chau, M.-H. Nematic Ordering of 4-n-Alkyl-4'-Cyanobiphenyls Studied by Carbon-13 NMR with Off-Magic-Angle Spinning. *J. Chem. Phys.* **1986**, *85*, 4808–4814.
- (48) Gan, Z. Spin Dynamics of Polarization Inversion Spin Exchange at the Magic Angle in Multiple Spin Systems. *J. Magn. Reson.* **2000**, *143*, 136–143.
- (49) Seed, A. Synthesis of Self-Organizing Mesogenic Materials Containing a Sulfur-Based Five-Membered Heterocyclic Core. *Chem. Soc. Rev.* **2007**, *36*, 2046–2069.
- (50) Amaranatha Reddy, R.; Tschierske, C. Bent-Core Liquid Crystals: Polar Order, Superstructural Chirality and Spontaneous Desymmetrisation in Soft Matter Systems. *J. Mater. Chem.* **2006**, *16*, 907–961.
- (51) Attard, G. S.; Date, R. W.; Imrie, C. T.; Luckhurst, G. R.; Roskilly, S. J.; Seddon, J. M.; Taylor, L. Non-Symmetric Dimeric Liquid Crystals The Preparation and Properties of the α -(4-cyanobiphenyl-4'-yloxy)- ω -(4-n-alkylanilinebenzylidene-4'-oxy) alkanes. *Liq. Cryst.* **1994**, *16*, 529–581.
- (52) Barbarin, F.; Dugay, M.; Piovesan, A.; Fadel, H.; Guillon, D.; Skoulios, A. Structural Study of the Smectic Phases of Several 4-cyanoalkoxybenzylidene-4'-alkylanilines. *Liq. Cryst.* **1987**, *2*, 815–823.
- (53) Hardouin, F.; Levelut, A. M.; Achard, M. F.; Sigaud, G. Polymorphism of Mesogenic Substances Containing Polar Molecules. Part I. Physical Chemistry and Structure. *J. Chim. Phys. Phys.-Chim. Biol.* **1983**, *80*, 53–64.
- (54) Prasad, V.; Lee, K.-H.; Park, Y. S.; Lee, J.-W.; Oh, D.-K.; Han, D. Y.; Jin, J.-I. Dimeric Compounds Containing Malonic Acid as the Central Linking Unit: Synthesis and Mesomorphic Properties. *Liq. Cryst.* **2002**, *29*, 1113–1119.
- (55) Hardouin, F.; Sigaud, G.; Keller, P.; Richard, H.; Tinh, N. H.; Mauzac, M.; Achard, M. F. Smectic A Polymorphism from Low to High Molar Mass Systems. *Liq. Cryst.* **1989**, *5*, 463–478.
- (56) Esselin, S.; Bosio, L.; Noel, C.; Decobert, G.; Dubois, J. C. Some Novel Smectic C* Liquid-Crystalline Side-Chain Polymers Polymethacrylates and Poly α -chloroacrylates. *Liq. Cryst.* **1987**, *2*, 505–518.
- (57) Tschierske, C., Ed. *Liquid Crystals: Materials Design and Self-Assembly*; Springer-Verlag: Berlin Heidelberg, 2012.